Supporting information

Jian Zhi[a,b*], Oliver Reiser[a], Youfu Wang[b], Aiguo Hu[b].

[a]Institute of Organic Chemistry, University of Regensburg, Universitätsstr.31,93053 Regensburg, Germany

[b]Shanghai Key Laboratory of Advanced Polymeric Materials, School of Materials Science and Engineering, East China University of Science and Technology, Shanghai 200237, China

Email: jian.zhi@outlook.com

Capacitance calculation

If the capacitances of the two electrodes, i.e. positive and negative, can be expressed as C_p and C_n, respectively, the overall capacitance (C_T) of the entire cell can be expressed as eqn (1):

$$\frac{1}{C_T} = \frac{1}{C_p} + \frac{1}{C_n} \quad (1)$$

In a symmetrical supercapacitor, C_p=C_n=C_0, where C_0 represents the per-electrode capacitance and in this study represents the capacitance of one electrode. So the relationship between C_T and C_0 should be as eqn (2):

$$C_0 = 2C_T = \frac{2It}{V} \quad (2)$$

where I, t and V are charged current, t is the discharge time, V is the voltage drop upon discharging (excluding IR drop).

As a result, the per-electrode areal capacitance (C_{A0}) and volumetric capacitance (C_{v0}) of the device is shown in eqn (3) and eqn (4):

$$C_{A0} = \frac{C_0}{A_0} = \frac{2It}{A_0} = \frac{4It}{A_T V} = 4C_{A-cell} \quad (3)$$

$$C_{v0} = \frac{C_0}{v_0} = \frac{2I(t - t_{OMC})}{v_0 V} = \frac{4I(t - t_{OMC})}{v_T V} = 4C_{v-cell} \quad (4)$$

Where A_0 is the surface area of in one electrode, which is approximately considered to be a cylinder. A_T represents the total mass the whole cell, in which A_T=2A_0. $C_{A\text{-}cell}$ is the areal capacity of the whole cell. V_0 is the volume of one electrode the total volume of the device

$v_t=2v_0$. $C_{v\text{-}cell}$ is the volumetric capacitance of the whole device.

The corresponding volumetric energy and power density are calculated through eqn (5) and (6):

$$E_v = \frac{1}{2}C_{v-cell}V^2 = \frac{1}{8}C_{v0}V^2 \qquad (5)$$

$$P_v = \frac{E_v}{t} \qquad (6)$$

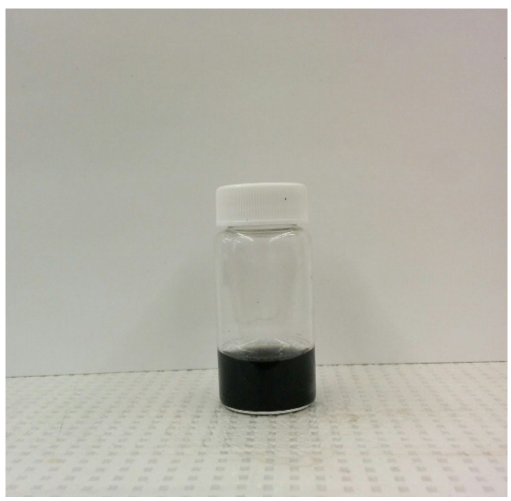

Figure S1. Digital image of a vial containing CVD gr/OMC dispersions stabilized by P123 surfactants.

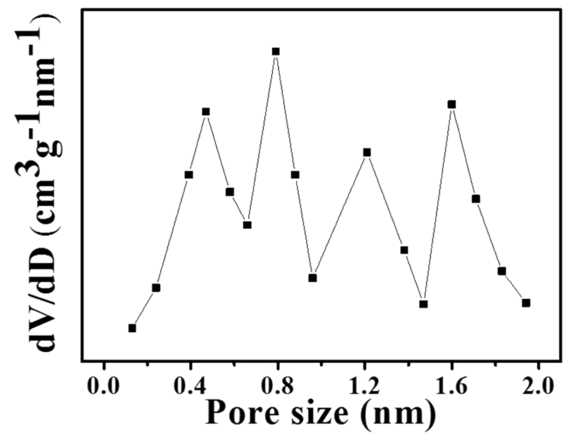

Figure S2. Pore size distribution of CVD gr/OMC below 2 nm calculated from the NLDFT model

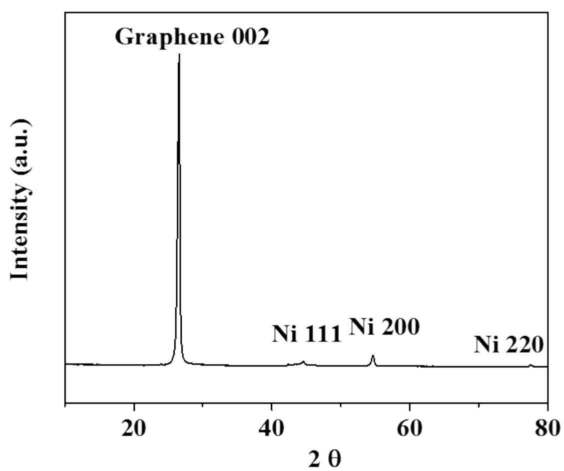

Figure S3. XRD pattern of CVD gr after Ni etching.

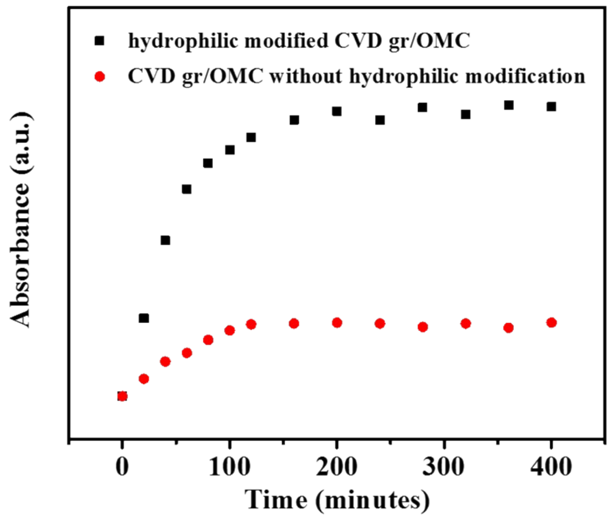

Figure S4. Absorbance at 660 nm measured for CVD gr/OMC dispersions as a function of sonication time.

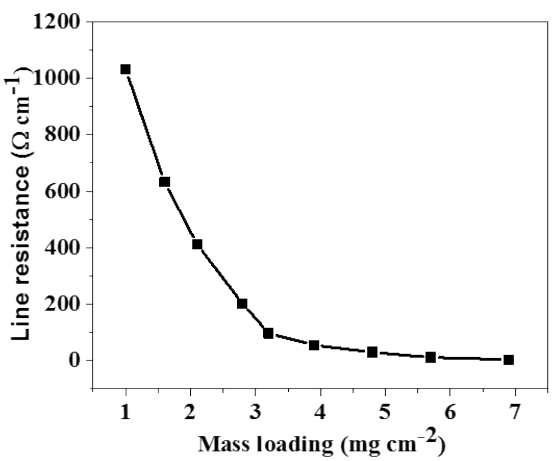

Figure S5. The relationship between line resistance and mass loading of CVD gr/OMC.

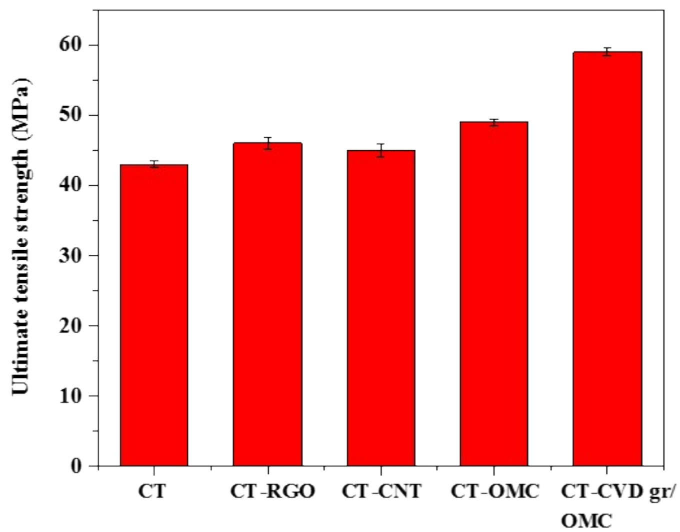

Figure S6. Ultimate tensile strength of various carbon coated cotton threads.

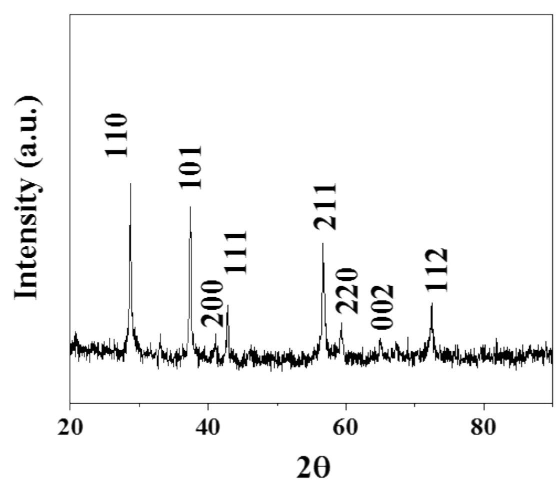

Figure S7. XRD patterns of MnO_2 spheres.

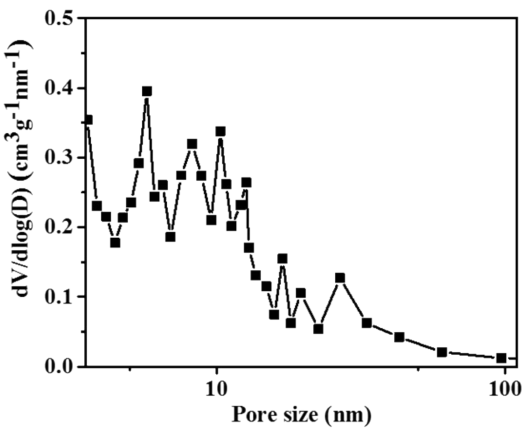

Figure S8. Bulk heterojunction (BJH) pore distribution spectra of the CT-CVD gr/OMC-MnO_2 composite electrode.

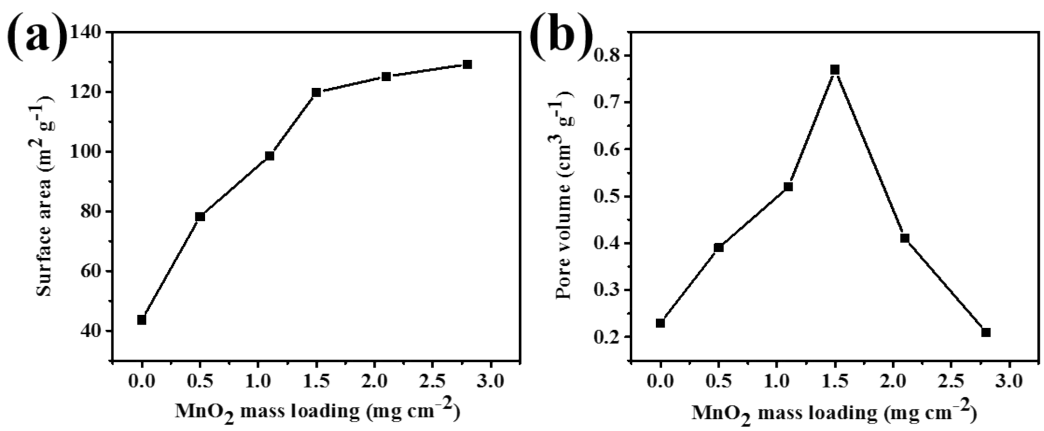

Figure S9. The relationship between surface area (a)/pore volume (b) and mass loading of MnO_2 nanoparticles on CT-CVD gr/OMC electrode.

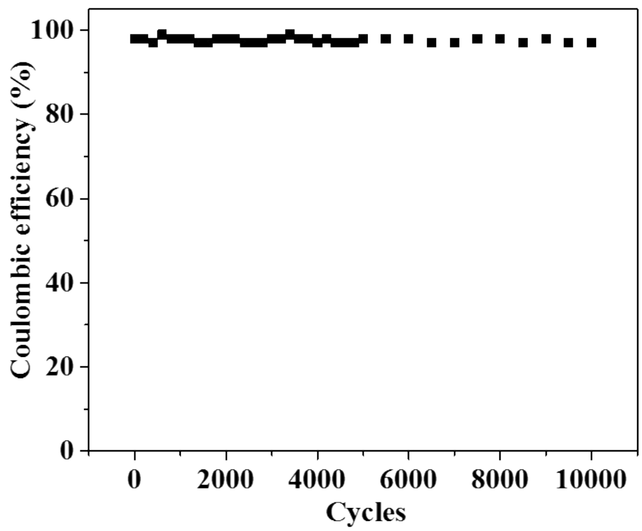

Figure S10. Coulombic efficiency of CT-CVD gr/OMC-MnO_2 supercapacitor as a function of cycling number at a current density of 13.76 mA cm^{-2}.

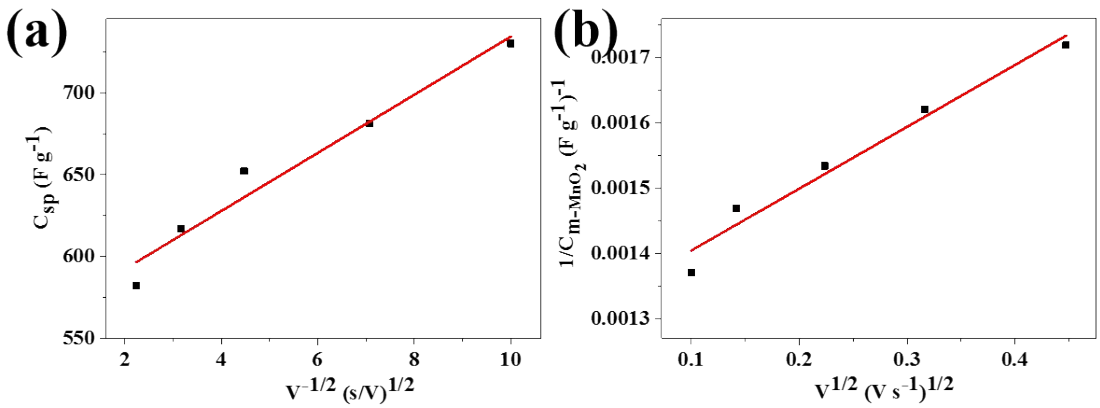

Figure S11. (a) Specific capacitance as a function of scan rate (inverse square root) for CT-CVD gr/OMC-MnO_2 electrode. (b) specific (inverse) capacitance as a function of scan rate (square root) for CT-CVD gr/OMC-MnO_2 electrode.

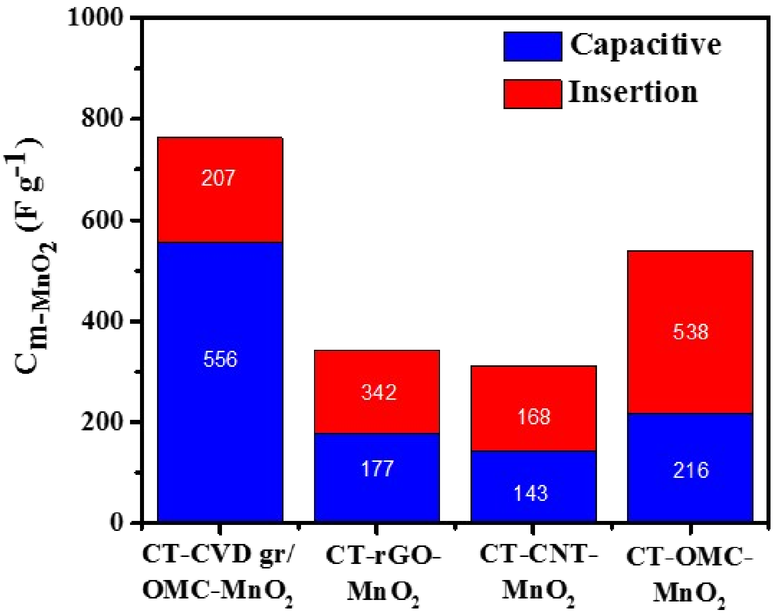

Figure S12. Bar graph of mass normalized capacitance of MnO2 in various thread-like supercapacitors with Faradaic insertion capacity (red) and Faradaic pseudocapacitive charging (blue) derived from Trasatti's method.

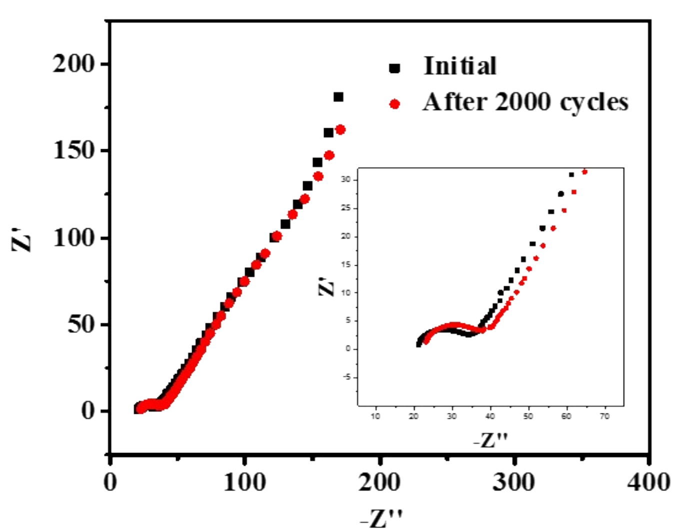

Figure S13. EIS spectra of CT-CVD gr/OMC supercapacitor before and after 3000 cycles.

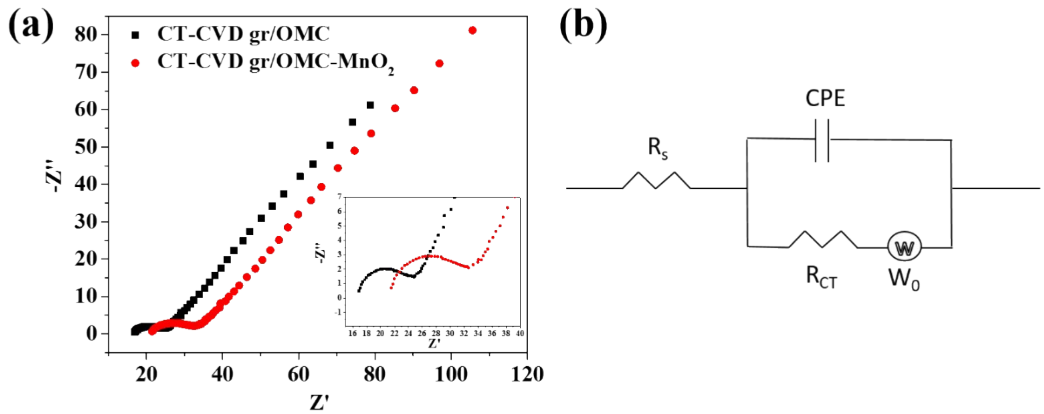

Figure S14 (a,b). EIS data of CT-CVD gr/OMC and CT-CVD gr/OMC- MnO_2 composites and the equivalent circuit diagram used for the fitting.

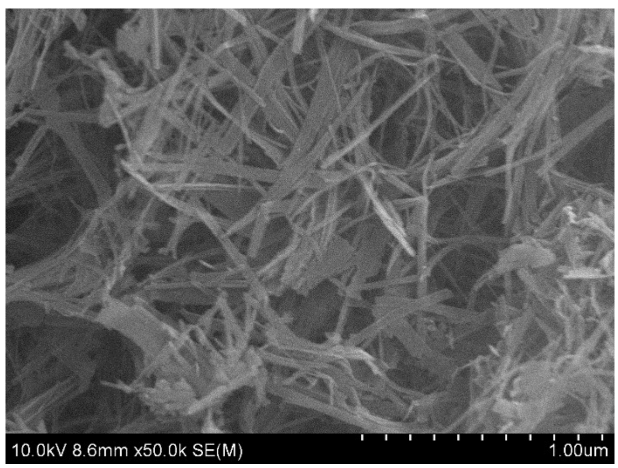

Figure S15. SEM image of TiO_2 nanowires

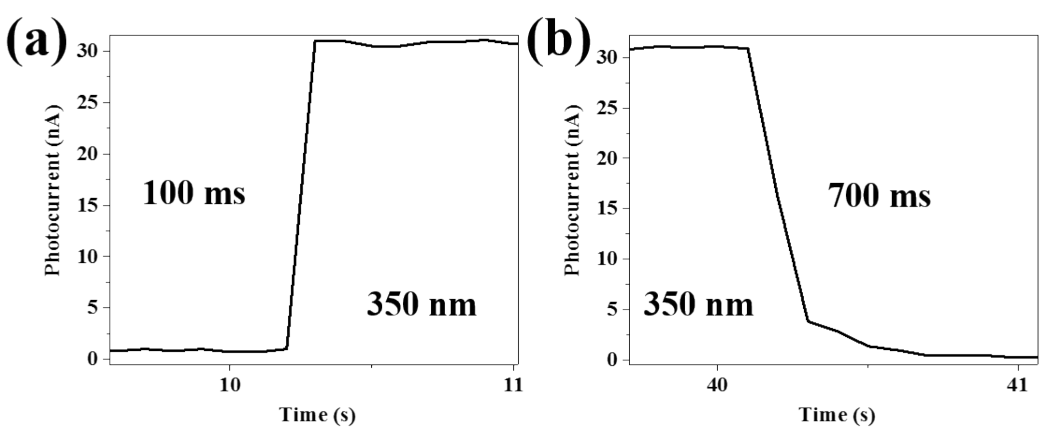

Figure S16. (a) Highlights of the response speed under 350 nm illumination. (b)

Highlights of the recovery speed under 350 nm illumination.

Table S1. Structural characterization data for CVD gr, OMC and CVD gr/OMC

Sample	BET-surface area (m^2 g^{-1})	Mesopore volume (cm^3 g^{-1})	Micropore volume (cm^3 g^{-1})	Micro/meso-porosity
CVD-gr	91	0.09	0	-
OMC	236	0.5	0.9	1.8
CVD-gr/OMC	328	0.4	1.1	2.8

Table S2. Comparison of electrochemical performance of yarn/fiber-based supercapacitors.

Ref.	Materials	Electrolyte	Voltage window	Pv mW cm^{-3}	Ev mWh cm^{-3}
73	PPy/ MnO_2/rGO	PVA/ H_3PO_4	0-0.8	16	1.1
16	ZnO/ MnO_2	PVA/LiCl	0-0.8	2.4	0.04
74	TiO_2/ MnO_2	PVA/LiCl	0-0.8	230	0.3
63	MnO_2/Carbon fiber	PVA/H_3PO_4	0-0.8	400	0.22
75	PPy	PVA/ H_3PO_4	0-0.8	270	1
15	PEDOT/CNT	PVA/ H_3PO_4	0-0.8	38000	1.1
76	WO_{3-x}/MoO_{3-x}	PVA/ H_3PO_4	0-1.9	730	1.9
77	Nickel fiber/Co_3O_4 nanowire	PVA/KOH	0-1.5	1470	0.62
78	$NiCo_2O_4$	PVA/KOH	0-1	17000	1.44
64	MnO_2/graphene/carbon fiber	PAAK/KCl	0-1.6	200	0.9
14	CuO/AuPd/ MnO_2	PVA/KOH	0-0.8	413	0.55
This work	CVD gr/OMC- MnO_2 cotton thread	PVA-BMIMCl-Li_2SO_4	0-1.5	300	2.7